

1 **EVOLVED GAS ANALYSIS-MASS SPECTROMETRY AND ISOCONVERSIONAL METHODS FOR THE**

2 **ESTIMATION OF COMPONENT-SPECIFIC KINETIC DATA IN WOOD PYROLYSIS**

3 Federica Nardella, Marco Mattonai, Erika Ribechini

4 Department of Chemistry and Industrial Chemistry, University of Pisa, Via G. Moruzzi 13, 56124 Pisa, Italy

5

6 **Abstract**

7 The pyrolysis reactions of hardwood and softwood were investigated using evolved gas analysis and mass
8 spectrometry (EGA-MS) and by treating the experimental data with isoconversional methods to obtain
9 kinetic information. Mass spectrometric detection allowed the identification of the pyrolysis products to be
10 performed and component-specific thermograms were obtained by the extraction of appropriate m/z
11 values without the need of peak-fitting. Finally, isoconversional methods, both an integral and a differential
12 method, were used on compound-specific thermograms to calculate apparent activation energies of the
13 carbohydrate and lignin fractions separately. The results showed that the two [isoconversional](#) methods
14 provide comparable results, and that there are significant differences between the energies of the
15 holocellulose and lignin fractions. This work shows that EGA-MS can provide reliable kinetic data for multi-
16 component samples without the need of chemical pre-treatments or signal deconvolution.

17

18 **Keywords:** Biomass; wood; isoconversional methods; evolved gas analysis; mass spectrometry

19

20

21 **1. INTRODUCTION**

22 Pyrolysis of lignocellulosic biomass has been thoroughly investigated in the past decades as a promising
23 source of sustainable fuels and highly valuable chemicals [1-4]. The complexity of biomass pyrolysis is such
24 that a sufficiently deep knowledge on the matter has not yet been obtained. In this frame, thermo-
25 analytical techniques have become tools of choice for the study of biomass pyrolysis, allowing us to
26 describe the composition of the pyrolysates and to obtain insights into the reaction mechanisms.

Codice campo modificato

27 Isoconversional methods are a group of macroscopic modelling methods which provide kinetic data about
28 complex systems [5-7]. Model-free isoconversional methods are a sub-category of such methods, that allow
29 us to estimate an apparent activation energy for a reaction without any assumption on its mechanism. An
30 estimation of the activation energy of a pyrolytic process can provide useful information on the energetics
31 of the process, guiding the optimization of conversion strategies. Isoconversional methods have been
32 extensively applied in the field of biomass pyrolysis to process data from thermogravimetric analysis (TGA)
33 and differential scanning calorimetry (DSC) [8-12].

Codice campo modificato

34 The main disadvantage of using TGA and DSC data is that isoconversional analysis of samples with more
35 than one component will yield information on the pyrolysis process of the whole system, without
36 information on the single components. This is particularly important when dealing with lignocellulosic
37 biomass, which is composed of a polysaccharidic fraction along with lignin, tannins and extractives.

Codice campo modificato

38 Two main strategies have been proposed in order to solve this problem. The first strategy is to consider
39 wood components individually, either by studying commercially available substrates or by separating the
40 components using traditional wet-chemistry methods [13-15]. Although separation techniques have been
41 fully optimized throughout the years, they always present the risk of modifying the polymeric structure of
42 lignocellulose components, resulting in different pyrolysis mechanisms and therefore different apparent
43 activation energies. For instance, it is known that extraction and purification of cellulose deeply affect both
44 its degree of polymerization and its crystallinity [16]. The second strategy is to perform the analysis of the
45 whole sample, and separate the contribution of each component to the total instrumental output by peak-
46 fitting [8,17]. This process does not entail sample pre-treatment, but requires approximation of each

Codice campo modificato

Codice campo modificato

Codice campo modificato

Codice campo modificato

47 degradation curve using specific mathematical expressions. This can be problematic when dealing with
48 natural polymers such as lignin, whose complex structure follows an intricate, multi-step pyrolysis
49 mechanism and generates degradation profiles which are hardly rationalized by analytical functions.
50 Recently, isoconversional analysis has been applied to evolved gas analysis-mass spectrometry (EGA-MS),
51 demonstrating that this technique can provide similar information to those obtained by TGA and DSC
52 [18,19]. Here, EGA-MS data obtained from the analyses of both softwood and hardwood samples were
53 treated with both differential and integral isoconversional methods. In EGA-MS, the pyrolysis products
54 evolved from each component of the sample can be monitored as a function of the furnace temperature in
55 a wide range of m/z values [20,21]. If a group of specific m/z values can be attributed to a single component
56 of the sample, then the extraction of these values from the total ion thermogram can be used to obtain
57 component-specific thermograms. Apparent activation energies are determined both from the total ion
58 thermogram, and from the thermograms obtained by selection of holocellulose- and lignin-specific m/z
59 values. Comparison of the activation energies are also carried out to discuss relations between the total
60 and component-specific activation energies. To the best of our knowledge, this is the first work dealing
61 with the study of whole lignocellulose using differential and integral isoconversional methods on both total
62 and extracted ion thermograms.

Codice campo modificato

Codice campo modificato

Codice campo modificato

Codice campo modificato

63

64 2. MATERIALS AND METHODS

65 2.1 Samples

66 Pine (*Pinus pinaster*), fir (*Abies alba*), oak (*Quercus petraea*) and iroko (*Milicia excelsa*) wood slabs were
67 obtained from a local provider. The slabs were mechanically reduced to splinters, and then the splinters
68 were ground to a fine powder using a Pulverisette 23 vibratory ball-mill (Fritsch,
69 Germany). The resulting particle size was measured with mechanical filters at various meshes and was
70 found to be approximately 0.2 mm. Before analysis, the powders were dried in oven at 60 °C for 8 h.
71 Approximately 50 µg of sample were used for each experiment.

72

73 **2.3 Experimental setup**

74 All experiments were performed with an EGA/PY-3030D micro-furnace pyrolyser (Frontier Laboratories
75 Ltd., Japan) coupled to a 6890 gas chromatograph equipped with a split/splitless injector and a 5973 mass
76 spectrometric detector (Agilent Technologies, USA). During each experiment, the furnace temperature was
77 raised from 100 to 700 °C at six different heating rates ($\beta = 15, 20, 25, 30, 35$ and 40 °C/min). The interface
78 between the furnace and the GC injector was kept at 100 °C above the furnace temperature, to a maximum
79 of 300 °C. The GC injector was operated in split mode with a 20:1 ratio at 280 °C. The pyrolyser and mass
80 spectrometer were connected by an Ultra ALLOY deactivated and uncoated stainless-steel capillary column
81 (UADTM-2.5N, 2.5 m x 0.15 mm, Frontier Laboratories Ltd, Japan), which was kept at 300 °C. Helium (1.2
82 mL/min) was used as carrier gas. The mass spectrometer was operated in EI positive mode (70 eV, m/z
83 range 50-300). The ion source and quadrupole analyzer were kept at 230 °C and 150 °C, respectively.

84 **2.4 Data processing**

85 The total and extracted thermograms at different heating rates for each sample were processed with
86 isoconversional methods. First, conversion profiles were calculated from the thermogram using (1), where
87 S is the total ion current of the mass spectrometer as a function of the temperature T , T_0 the initial
88 temperature, and A_{TOT} is the total area of the thermogram.

$$89 \quad (1) \quad \alpha = \frac{1}{A_{TOT}} \int_{T_0}^T S(\tau) d\tau$$

90 Both the differential and the Kissinger-Akahira-Sunose isoconversional methods were used. The equations
91 for these two methods are (2) and (3), respectively, where α is the conversion, β is the heating rate, E_a the
92 activation energy, R the gas constant, and $q(\alpha)$ and $r(\alpha)$ are functions of the conversion. For a fixed value of
93 α , both these equations give a linear trend of the left side as a function of $1/T$. The slope of these functions
94 can be directly related to the activation energy.

$$95 \quad (2) \quad \ln \left(\beta \frac{d\alpha}{dT} \right) = -\frac{E_a}{RT} + q(\alpha)$$

96 (3) $\ln\left(\frac{\beta}{T^2}\right) = -\frac{E_a}{RT} + r(\alpha)$

97 The derivative of the conversion to be used in (2) was calculated using the definition of conversion given in
98 (1), as shown in (4). Equation (4) shows that the derivative of conversion can be calculated directly from the
99 total ion current S of the mass spectrometer, without requiring derivation. This is an important advantage
100 of EGA-MS over TGA, as derivation usually results in a decrease of the signal to noise ratio and introduces
101 significant error in the calculation 5.

102 (4) $\frac{d\alpha}{dT} = \frac{1}{A_{TOT}} \frac{d}{dT} \int_{T_0}^T S(\tau) d\tau = \frac{S(T)}{A_{TOT}}$

103 Reproducibility of the EGA-MS experiments was established by repeating the analysis of the same sample
104 at the same heating rate for three times. The relative standard deviation, calculated on the total
105 thermogram area divided by the sample amount, was found to be less than 10%.

106

107 3. RESULTS AND DISCUSSION

108 3.1 EGA-MS

109 Figure 1 shows the total ion thermograms obtained for pine and oak, which are representative of a
110 softwood and a hardwood, respectively. The associated average mass spectra are also shown.

111 The lower m/z ratios in the mass spectra (m/z 57, 60, 69, 73, 85, 98, 114) can be related to the pyrolysis
112 products of the polysaccharidic fraction of the wood, while the higher ratios (m/z 137, 151, 164, 167, 181)
113 are ascribable to the lignin thermal degradation. The structures of the fragment ions responsible for the
114 main MS peaks are displayed in Table 1.

115 The ions giving signals at m/z 60, 69 and 73 are obtained by fragmentation reactions involving the
116 monosaccharides of holocellulose [22]. These fragmentations can take place following various mechanisms,
117 including extrusions, retro-aldol condensation and retro-Diels-Alder reactions. Fragmentation of

Codice campo modificato

ha formattato: Tipo di carattere: Corsivo

Codice campo modificato

118 monosaccharides in either their linear or cyclic forms is favored by the formation of a double bond
119 following dehydration, which is one of the main reactions during the pyrolysis of polysaccharides [23,24].
120 The ions at m/z 60 and 73, in particular, originate from levoglucosan which is the most characteristic
121 pyrolysis product of cellulose [25,26].

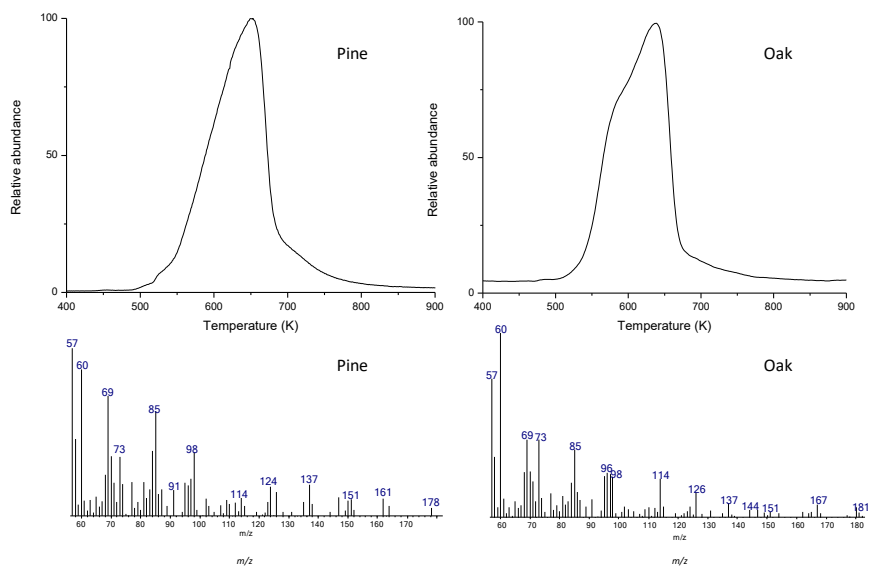
Codice campo modificato

Codice campo modificato

Codice campo modificato

Codice campo modificato

122



123

124 **Figure 1** – Top: Total ion thermograms obtained for (left) pine wood and (right) oak wood at $\beta = 20$ °C/min.

125 Bottom: average mass spectra from the EGA profiles of (left) pine and (right) oak.

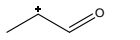
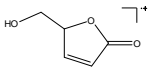
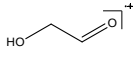
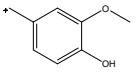
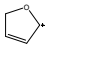
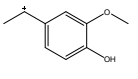
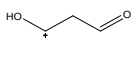
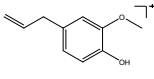
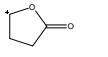
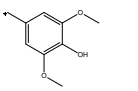
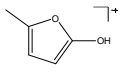
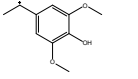
126

127

128

129

130 **Table 1** – Structures of the fragment ions deriving from holocellulose and lignin.

| <i>m/z</i> | Structure | Component | <i>m/z</i> | Structure | Component |
|------------|---|-----------|------------|---|-----------|
| 57 |  | H | 114 |  | H |
| 60 |  | H | 137 |  | L |
| 69 |  | H | 151 |  | L |
| 73 |  | H | 164 |  | L |
| 85 |  | H | 167 |  | L |
| 98 |  | H | 181 |  | L |

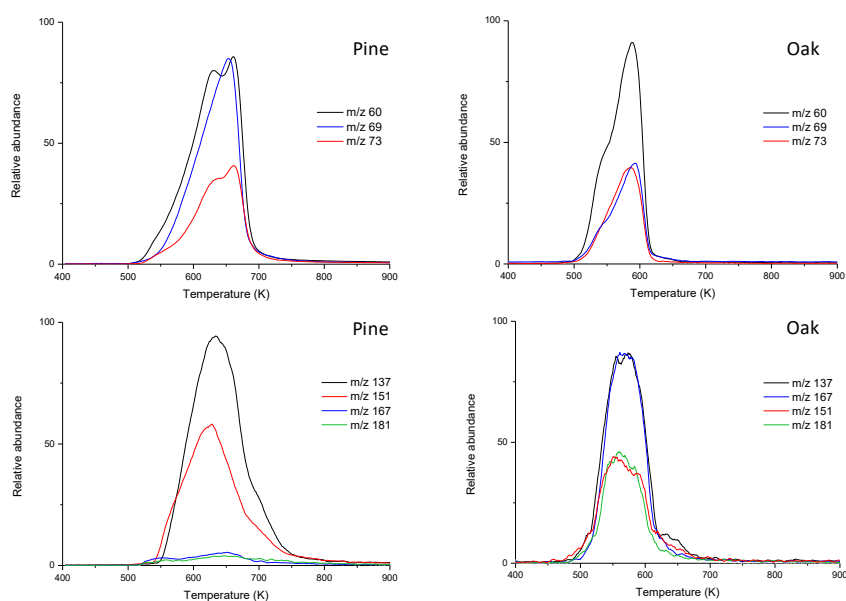
131

132 The signals at *m/z* 137, 151 and 164 are characteristic of guaiacyl alcohol monomers, which are obtained
 133 from depolymerization of both softwood and hardwood lignin during pyrolysis, while the peaks at *m/z* 167
 134 and 181 are characteristic of syringyl alcohol monomers, only present in hardwood lignin. The characteristic
 135 signals of lignin correspond to its monomers, generated from depolymerization, which have undergone a
 136 partial fragmentation of the propanoid side chain. The ions at *m/z* 137 and 167 are obtained after loss of
 137 two carbon atoms from the side chain, while those at *m/z* 151 and 181 are obtained after the loss of a
 138 single carbon atom [27,28].

139 In order to separate the contribution of holocellulose and lignin we extracted the main *m/z* signals
 140 representative of both holocellulose and lignin from the total ion thermograms: *m/z* 60, 69 and 73 for
 141 holocellulose, *m/z* 137, 151, 167 and 181 for lignin. The extracted ion profiles are displayed in Figure 2.

Codice campo modificato

Codice campo modificato



143

144 **Figure 2** – Extracted ion profiles for (top) holocellulose and (bottom) lignin from the thermograms of pine
 145 wood and oak wood recorded at $\beta = 20 \text{ }^\circ\text{C/min}$.

146

147 The extracted ion profiles of holocellulose for both hardwood and softwood presented a shoulder peak at
 148 lower temperatures and a main peak at high temperatures, which can be attributed to the pyrolysis
 149 processes of hemicellulose and cellulose, respectively [29]. The extracted ion profiles of lignin showed two
 150 peaks as well, which are particularly evident in the extracted ion thermograms of pine wood. Contrary to
 151 holocellulose, these two peaks do not correspond to the pyrolysis of different fractions of lignin, but to
 152 different stages in the pyrolysis process. In fact, lignin pyrolysis is known to follow an extremely complex
 153 mechanism, with degradation reactions affecting first the alkyl side chains of the monomers, and then the
 154 hydroxy and methoxy groups on the aromatic rings [30,31].

Codice campo modificato

Codice campo modificato

Codice campo modificato

155 As expected, the abundance of the signal at m/z 167 and 181 for pine wood is very low due to the low
156 amount of syringyl-lignin in softwoods, while all four m/z signals provided significant peak heights in the
157 case of oak wood. [The total ion thermograms of all the samples considered are provided in Figure S1 in the](#)
158 [Supplementary Materials along with their compound-specific thermograms for](#)
159 [holocellulose and lignin.](#)

160

161 3.2 Isoconversional methods

162 Both differential and Kissinger-Akahira-Sunose isoconversional methods were used to calculate apparent
163 activation energies from the EGA-MS thermograms. In addition to the total ion thermogram, two fraction-
164 specific thermograms were obtained by extracting the discussed m/z signals. The m/z signals were chosen
165 based on their relative intensities in the mass spectra and their representativeness of the corresponding
166 fraction of wood.

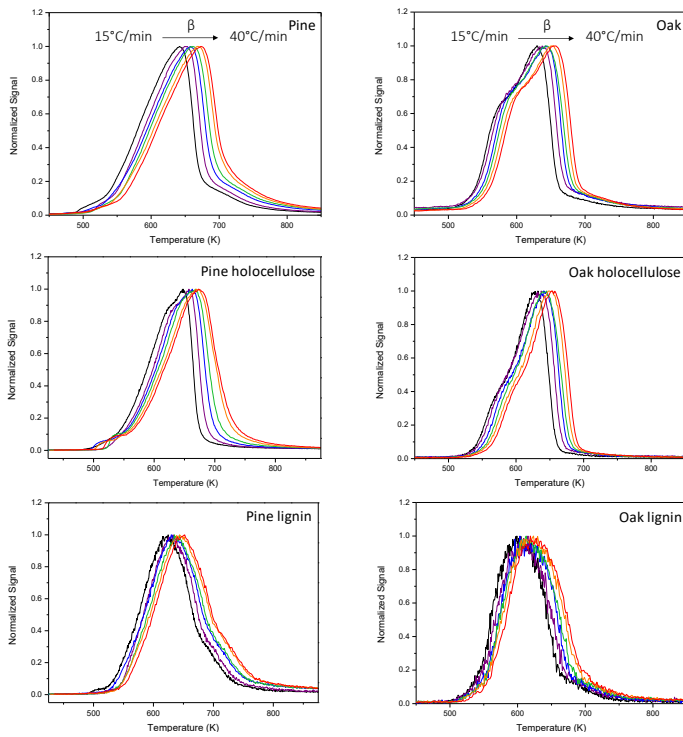
167 The m/z signals at 60, 69 and 73 were extracted and summed to obtain a holocellulose-specific
168 thermogram, while the m/z signals at 137, 151, 167 and 181 were used to obtain a lignin-specific
169 thermograms. Normalized total ion thermograms and compound-specific thermograms at all heating rates
170 for both pine and oak wood are displayed in Figure 3. [Although a small number of \$m/z\$ values was selected](#)
171 [for each compound-specific thermogram, well-defined profiles were obtained in most of the cases. The](#)
172 [only exception to this was oak lignin, which provided a relatively low signal-to-noise ratio. This is most likely](#)
173 [due to a low content of lignin in this hardwood sample.](#)

174 Once the series of thermograms was obtained, the extent of conversion α was calculated using (1). Figure 5
175 shows the conversion profiles obtained for pine wood and oak wood at all heating rates.

176 Once the conversion profiles were determined, six conversion values (from $\alpha=0.2$ to $\alpha=0.7$ with intervals of
177 0.1) were chosen, for each sample, to perform linear regression. [We selected this range of values because](#)
178 [of the background noise existing in the thermograms, in particular in the extracted ion thermograms. The](#)
179 [presence of the noise can affect the results at limit values of conversion, providing high standard deviations](#)

180 and improper interpretation of the data. The obtained conversion profiles are presented in Figure 4. Figure
181 5 and Figure 6 show the regression curves obtained for pine and oak woods and their components, using
182 the KAS method and the differential method respectively.

183

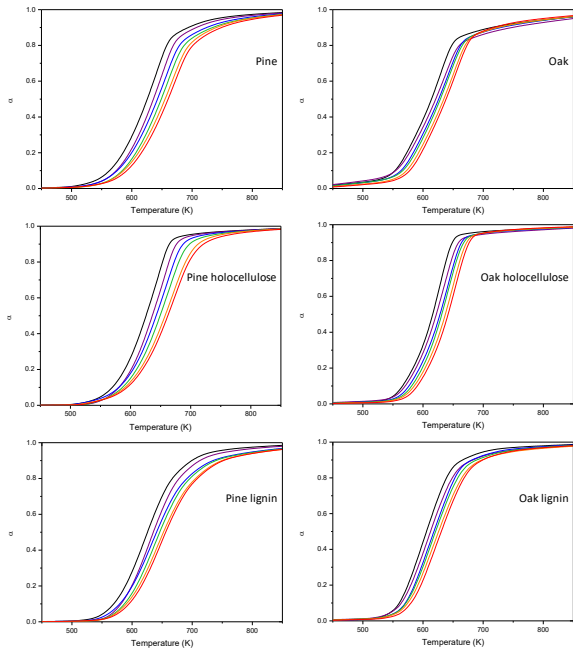


184

185 **Figure 3** – Normalized thermograms obtained by EGA-MS for pine and oak raw wood, holocellulose and
186 lignin at different heating rates (15, 20, 25, 30, 35, 40 °C/min).

187

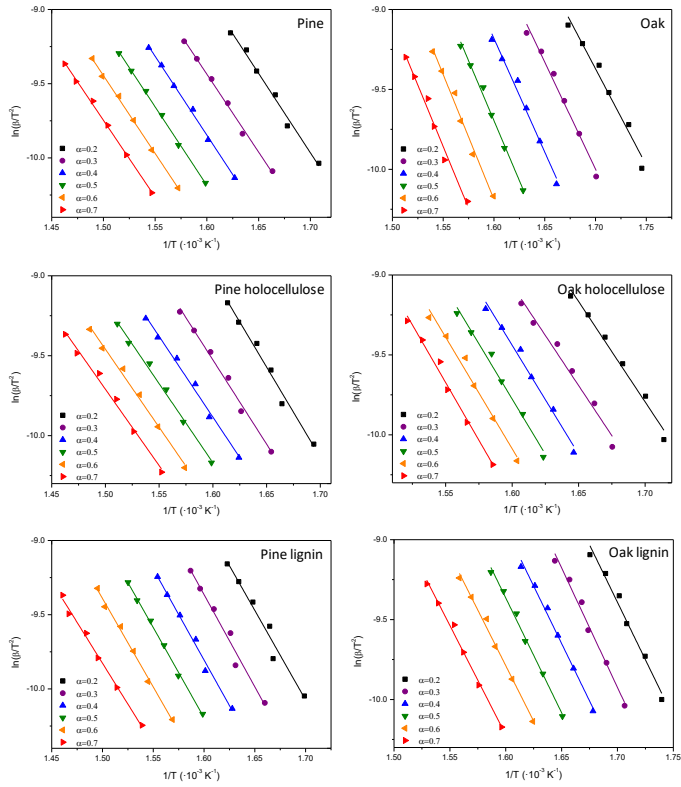
188



189

190 **Figure 4** – Conversion profiles obtained for (left) pine wood and (right) oak wood and their component.

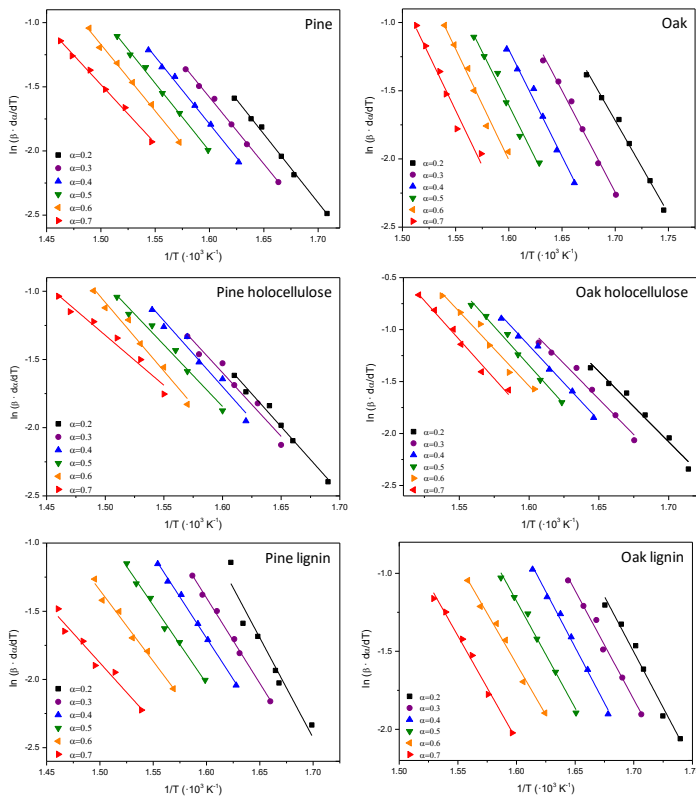
191



192

193 **Figure 5** – Linear regression curves obtained using the KAS method for (left) pine and (right) oak woods and
 194 their components.

195



196

197 **Figure 6** – Linear regression curves obtained using the differential method for (left) pine and (right) oak
 198 woods and their components.

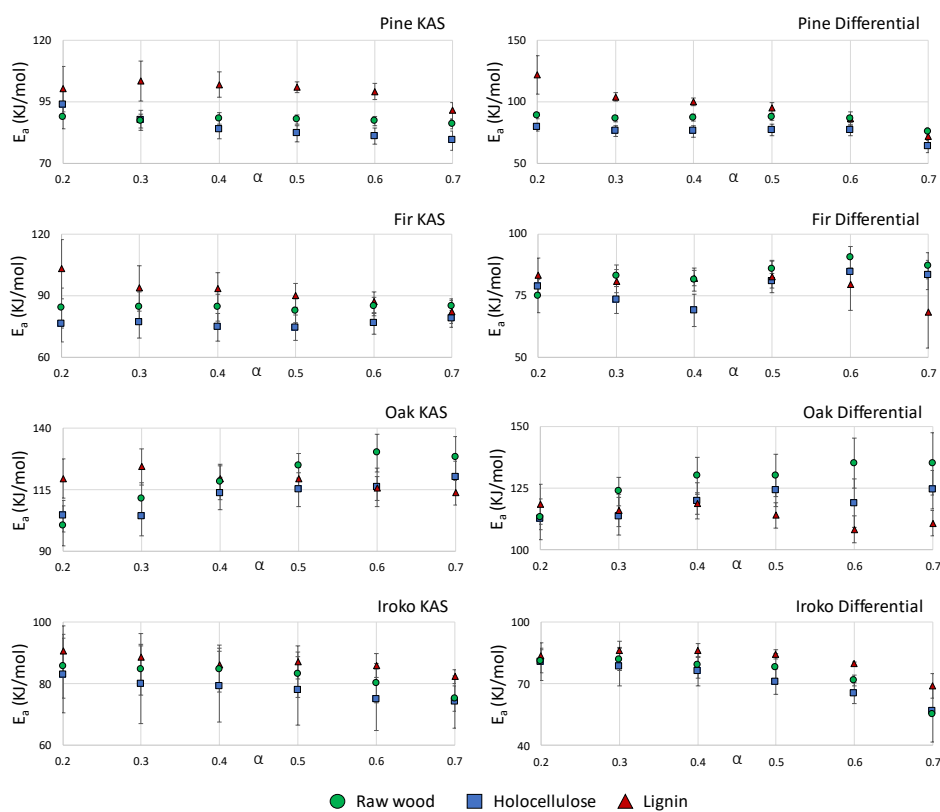
199

200 Graphical trends of the results apparent activation energies obtained for all wood samples are shown in
 201 Figure 7. Oak wood showed the highest values of apparent activation energy and was the only case in
 202 which these values increased with the increase of the conversion. The activation energies obtained for the
 203 other woods tended to decrease as α increased. Significant variations of E_a can be observed between the
 204 lowest and the highest conversion values selected ($\alpha=0.2$ and $\alpha=0.7$). In only a few cases, the changes in
 205 the E_a values calculated with the KAS method fall within the estimated uncertainties, but overall, we can
 206 state that the activation energy varies with the extent of conversion. The observed trends are likely due to

207 an interaction between the pyrolysis products and the substrate, which can modify the reaction mechanism
208 and therefore the corresponding activation energy as the temperature raises [5].

Codice campo modificato

209



210

211 **Figure 7** – Apparent activation energy values as a function of conversion for pine, fir, oak and iroko and
212 their fractions obtained with (left) KAS and (right) differential methods.

213

214 The values of the apparent activation energies measured for the lignin component are higher on average
215 than those calculated for the raw wood and the holocellulose component. This was expected, as lignin is
216 the most thermally resistant component of wood and its degradation occurs at higher temperatures than

217 the degradation of holocellulose. This is also confirmed by the temperature values of the holocellulose and
218 lignin-specific thermograms in Figure 3.

219 The six slopes obtained from the regression curves were averaged to estimate the activation energies. The

220 results obtained for [all wood samples](#) are shown in Table 2

221 .

222

223 **Table 2** – Apparent activation energies and R² values obtained by linear regression using KAS and

224 differential isoconversional methods on EGA-MS data; H: holocellulose; L: lignin.

| | KAS E _a (KJ/mol) | KAS average R ² | Differential E _a (KJ/mol) | Differential average R ² |
|----------------|-----------------------------|----------------------------|--------------------------------------|-------------------------------------|
| Pine | 88 ± 1 | 0.988 | 85 ± 5 | 0.992 |
| Pine H | 85 ± 5 | 0.987 | 75 ± 6 | 0.974 |
| Pine L | 100 ± 4 | 0.973 | 97 ± 20 | 0.968 |
| Fir | 84 ± 1 | 0.976 | 84 ± 5 | 0.979 |
| Fir H | 76 ± 2 | 0.981 | 78 ± 6 | 0.987 |
| Fir L | 92 ± 7 | 0.952 | 79 ± 6 | 0.938 |
| Oak | 119 ± 10 | 0.986 | 128 ± 8 | 0.983 |
| Oak H | 112 ± 6 | 0.976 | 119 ± 5 | 0.977 |
| Oak L | 119 ± 4 | 0.981 | 114 ± 4 | 0.980 |
| Iroko | 82 ± 4 | 0.967 | 74 ± 10 | 0.950 |
| Iroko H | 78 ± 3 | 0.933 | 71 ± 9 | 0.951 |
| Iroko L | 87 ± 3 | 0.967 | 82 ± 7 | 0.986 |

225

226 [It is important to notice that, despite the lower signal-to-noise ratio, the relative standard deviation on the](#)

227 [apparent activation energy and average R² of oak lignin were comparable with those obtained from the](#)

228 [other thermograms.](#) The average activation energies obtained with the two methods were compared using

229 the Student's *t*-test and Welch's test at a 95% confidence. The differences between E_a values proved to be

230 statistically negligible in most of the cases. For pine holocellulose and fir lignin the values obtained with the

231 two methods result to be statistically different. These results suggest that the differential and integral

232 isoconversional methods can both be used to obtain reliable kinetic data on the pyrolysis process of wood.

233 In particular, EGA-MS allows us to use the differential method with the advantage of calculating $d\alpha/dT$

234 directly from the experimental data, without performing any derivation. This is particularly interesting, as
235 the differential method estimates the activation energy without any mathematical approximation.
236 The obtained apparent activation energy values were compared with those available in the literature
237 calculated from TGA experiment [13,32-38]. Data present in literature are summarized in Table S1 of the
238 Supplementary Materials. In several cases the average energies measured in our work result to be lower
239 than the values reported in the literature. For instance, Yao and co-workers reported a value of 160 KJ/mol
240 for pine wood using the KAS method[33], while Park et al. determine the activation energy for oak trees in
241 the range of 216 – 461 KJ/mol by the differential method [36]. Both the works employ samples with particle
242 size around 0.8 mm. The difference could be due to the heat transfer to the sample. since it's well known
243 that the particles size influences the heat transfer process [39]. If the heat supply is not efficient
244 it could lead to slow pyrolysis and incomplete reactions, the temperature in the sample at any given point
245 during the experiment can be lower than the nominal temperature, resulting in an overestimation of the
246 degradation temperature and therefore a greater apparent activation energy. Thanks to the smaller sample
247 amount and particle size, heat transfer in EGA experiment is more efficient than in TGA, and this means
248 that the degradation temperature is reached at slightly lower times in our experimental setup. In some
249 cases, the difference in the results is could also be due to other factors, such as the plant species and
250 origin as well as the sampling point. Furthermore, the energy values reported for lignin were lower than
251 those reported for cellulose and hemicellulose, in contrast to our results. This can be attributed to the
252 significant chemical changes in the native structure of lignin, that could have been introduced with during
253 its isolation *via* chemical methods from the whole biomass, and taking into account that the thermal
254 stability of lignin depends on the isolation method and the plant species.

Codice campo modificato

256 4. CONCLUSIONS

257 In the present work, the pyrolysis of four wood species using EGA-MS and model-free isoconversional
258 methods was investigated for the first time. Selection of specific *m/z* values allowed us to obtain
259 cumulative extracted ion thermograms that were used as representative of the polysaccharide and lignin

260 fractions of wood. Model-free isoconversional methods provided apparent activation energy values for the
261 whole wood as well as for the single components, and these values were found to be ~~slightly~~ lower than
262 those obtained from TGA data.

263 The main advantages of EGA-MS as a technique for kinetic analysis were outlined in the paper. This
264 technique requires small sample amounts, ensuring an efficient heat transfer from the system to the
265 sample. If compound-specific m/z values are found in the mass spectrum of the thermogram, this
266 technique can also provide information on the single components of wood, without the need of curve-
267 fitting of the data or extraction of the components using wet chemistry methods. Moreover, EGA-MS
268 allows the application of differential isoconversional method, which does not require approximations,
269 without the need of derivation of the experimental data.

270 We believe the results of the present work prove that EGA-MS can be a useful tool for the kinetic analysis
271 of lignocellulose pyrolysis. In addition, the possibility of obtaining component-specific thermograms could
272 be applied in the future to study the co-pyrolysis of biomass with other substrates such as plastics, which is
273 a research field of growing interest.

274

275 ACKNOWLEDGEMENTS

276 The authors would like to acknowledge the University of Pisa for having funded the
277 project “Advanced analytical pyrolysis to study polymers in renewable energy, environment, cultural
278 heritage” (PRA_2018_26).

279 The authors would also like to thank the project “Heterogeneous Robust Catalysts to Upgrade Low value
280 biomass Streams (HERCULES)” funded by the Italian Ministry of Education, Universities and Research
281 (MIUR) within PRIN 2015 call.

282

283 REFERENCES

- 284 [1] S. Wang, G. Dai, H. Yang and Z. Luo, *Progress in Energy and Combustion Science*, 62, (2017) 33.
285 [2] G. SriBala, H.H. Carstensen, K.M. Van Geem and G.B. Marin, *Wiley Interdisciplinary Reviews: Energy*
286 *and Environment*, 8, (2019) e326.

- 287 [3] M. Uddin, K. Techato, J. Taweekun, M.M. Rahman, M. Rasul, T. Mahlia and S. Ashrafur, *Energies*, 11,
288 (2018) 3115.
- 289 [4] G. Kabir and B. Hameed, *Renewable and Sustainable Energy Reviews*, 70, (2017) 945.
- 290 [5] S. Vyazovkin, *Isoconversional kinetics of thermally stimulated processes*, Springer, 2015, p.
- 291 [6] S. Vyazovkin, A.K. Burnham, J.M. Criado, L.A. Pérez-Maqueda, C. Popescu and N. Sbirrazzuoli,
292 *Thermochimica Acta*, 520, (2011) 1.
- 293 [7] P. Šimon, *Journal of Thermal Analysis and Calorimetry*, 76, (2004) 123.
- 294 [8] I. Ali, H. Bahaitham and R. Naebulharam, *Bioresource Technology*, 235, (2017) 1.
- 295 [9] A. Anca-Couce, A. Berger and N. Zobel, *Fuel*, 123, (2014) 230.
- 296 [10] Y.J. Rueda-Ordóñez and K. Tannous, *Bioresource technology*, 196, (2015) 136.
- 297 [11] P.E. Sánchez-Jiménez, L.A. Pérez-Maqueda, A. Perejón, J. Pascual-Cosp, M. Benítez-Guerrero and
298 J.M. Criado, *Cellulose*, 18, (2011) 1487.
- 299 [12] M.A. Mehmood, G. Ye, H. Luo, C. Liu, S. Malik, I. Afzal, J. Xu and M.S. Ahmad, *Bioresource*
300 *Technology*, 228, (2017) 18.
- 301 [13] G. Jiang, D.J. Nowakowski and A.V. Bridgwater, *Thermochimica Acta*, 498, (2010) 61.
- 302 [14] G. Lv and S. Wu, *Journal of Analytical and Applied Pyrolysis*, 97, (2012) 11.
- 303 [15] J.B. Dahiya, K. Kumar, M. Muller-Hagedorn and H. Bockhorn, *Polymer International*, 57, (2008) 722.
- 304 [16] A.C. O'Sullivan, *Cellulose*, 4, (1997) 173.
- 305 [17] P. Brachi, F. Miccio, M. Miccio and G. Ruoppolo, *Fuel Processing Technology*, 154, (2016) 243.
- 306 [18] Y.-M. Kim, T.U. Han, B. Hwang, Y. Lee, A. Watanabe, N. Teramae, S.-S. Kim, Y.-K. Park and S. Kim,
307 *Polymer Testing*, 60, (2017) 12.
- 308 [19] M. Mattonai, D. Pawcenis, S. del Seppia, J. Łojewska and E. Ribechini, *Bioresource Technology*, 270,
309 (2018) 270.
- 310 [20] R. Risoluti and S. Materazzi, *Applied Spectroscopy Reviews*, 54, (2019) 87.
- 311 [21] S. Materazzi, A. Gentili and R. Curini, *Talanta*, 69, (2006) 781.
- 312 [22] T. Hosoya, H. Kawamoto and S. Saka, *Journal of analytical and applied pyrolysis*, 80, (2007) 118.
- 313 [23] J.B. Paine III, Y.B. Pithawalla and J.D. Naworal, *Journal of Analytical and Applied Pyrolysis*, 82, (2008)
314 42.
- 315 [24] G.C. Galletti and P. Bocchini, *Rapid communications in mass spectrometry*, 9, (1995) 815.
- 316 [25] D. Shen, W. Jin, J. Hu, R. Xiao and K. Luo, *Renewable and Sustainable Energy Reviews*, 51, (2015)
317 761.
- 318 [26] X. Zhang, W. Yang and C. Dong, *Journal of Analytical and Applied Pyrolysis*, 104, (2013) 19.
- 319 [27] D. Shen, S. Gu, K. Luo, S. Wang and M. Fang, *Bioresource Technology*, 101, (2010) 6136.
- 320 [28] S. Wang, K. Wang, Q. Liu, Y. Gu, Z. Luo, K. Cen and T. Fransson, *Biotechnology Advances*, 27, (2009)
321 562.
- 322 [29] D. Tamburini, J.J. Łucejko, E. Ribechini and M.P. Colombini, *Journal of Mass Spectrometry*, 50,
323 (2015) 1103.
- 324 [30] T. Kotake, H. Kawamoto and S. Saka, *Journal of analytical and applied pyrolysis*, 105, (2014) 309.
- 325 [31] T. Kotake, H. Kawamoto and S. Saka, *Journal of Analytical and Applied Pyrolysis*, 113, (2015) 57.
- 326 [32] C. Di Blasi, *Fast pyrolysis of biomass: a handbook*, 3, (2005) 121.
- 327 [33] F. Yao, Q. Wu, Y. Lei, W. Guo and Y. Xu, *Polymer Degradation and Stability*, 93, (2008) 90.
- 328 [34] A. Anca-Couce, N. Zobel, A. Berger and F. Behrendt, *Combustion and Flame*, 159, (2012) 1708.
- 329 [35] F. Thurner and U. Mann, *Industrial & Engineering Chemistry Process Design and Development*, 20,
330 (1981) 482.
- 331 [36] Y.-H. Park, J. Kim, S.-S. Kim and Y.-K. Park, *Bioresource Technology*, 100, (2009) 400.
- 332 [37] D.Q. Tran and C. Rai, *Fuel*, 57, (1978) 293.
- 333 [38] Q. Liu, S. Wang, Y. Zheng, Z. Luo and K. Cen, *Journal of Analytical and Applied Pyrolysis*, 82, (2008)
334 170.
- 335 [39] M. Van de Velden, J. Baeyens, A. Brems, B. Janssens and R. Dewil, *Renewable energy*, 35, (2010)
336 232.

337

